


Matching Rates and Optimal Allocation for Federated Probe-Logit Distillation under Heterogeneous Bandwidth Budgets

Prasanjit Dubey  Xiaoming Huo 

H. Milton Stewart School of Industrial and Systems Engineering,
Georgia Institute of Technology, Atlanta, GA 30332, U.S.A.

Abstract

High-stakes applications (multi-hospital clinical networks, multi-tenant enterprise knowledge bases, scientific consortia) would benefit from a language model trained on data scattered across nodes that cannot pool their data and cannot exchange gradients or weights at full precision. We study a basic statistical question this regime poses: at what minimax rate can a discrete conditional distribution over V tokens be estimated from K nodes each holding n samples, when each node may upload at most B bits per query in a public probe set? *Federated probe-logit distillation* (FPLD) is the canonical analytical vehicle: each node transmits a scalar-quantized logit vector on the probe set, and an aggregator distills a global parametric student. Prior work [Dubey and Huo, 2026] establishes a high-probability KL rate of the form $O(d/(Kn) + \rho\sqrt{V \log V/m} + K^{-1} \cdot 2^{-2B/V})$ plus optimization slack, with the bandwidth term in its softmax-Hessian-trace-sharpened form (Lemma B.7). We recap this result as Theorem 3.1. The three terms have classical statistical readings (pooled-MLE, probe-empirical-process, and a new communication-distortion piece); whether the bandwidth term is rate-optimal, and how the upper bound generalizes to heterogeneous per-node bandwidths, are left open in that work.

We close both gaps. First, the dithered FPLD construction has a matching single-round lower bound $\Omega(K^{-1} \cdot 2^{-2B/V})$ under non-degeneracy (Theorem 4.2), pinning the bandwidth-axis rate of the construction at $\Theta(K^{-1} \cdot 2^{-2B/V})$. T -round sequential refinement with nested/scaled residual quantizers sharpens the achievable rate to $O(K^{-1} \cdot 2^{-2TB/V})$ (Theorem 4.3); vanilla FPLD’s bandwidth term is T -independent and is therefore strictly suboptimal for every $T > 1$, a protocol-design improvement available within the same scalar-quantization channel. Second, we establish a heterogeneous-bandwidth upper bound for per-node budgets B_i , paired with a closed-form optimal allocation of log-tilted water-filling shape $B_i^* = B_{\text{tot}}/K + (V/2) \log_2(w_i/\bar{w}_g)$, the per-node analogue of reverse water-filling for distortion-rate optimization. A plug-in adaptive variant estimates the weights from a short warm-up phase and attains $1 + O(\sqrt{\log(K/\delta)/(mT_0)})$ relative suboptimality. Synthetic n-gram simulations confirm that empirical KL is bracketed by the upper and lower bounds and that the optimal allocation strictly dominates uniform and inverse-weighted baselines under heterogeneous clipping.

1 Introduction

A growing class of high-stakes applications would benefit from a language model trained on data that cannot be centralized (regulation, consent, institutional policy) and exchanged over uplinks too narrow to carry full-precision gradients or weights. As a running example, each hospital in a clinical consortium fine-tunes a small local language model (weak in isolation) on its private patient records and exchanges only bandwidth-limited summaries over an existing low-rate WAN. Prior work [Dubey and Huo, 2026] sets up the full pipeline (federated training plus inference-time conformal coverage) and proves a high-probability KL-consistency rate for the *Federated Probe-Logit Distillation* (FPLD) training-time protocol, in which each node transmits scalar-quantized logits on a public probe set and the aggregator distills a global parametric student.

Statistical reading of the rate. The FPLD upper bound recapped in Section 3 (Theorem 3.1) takes the form $O(d/(Kn) + \rho\sqrt{V \log(V/\delta)/m} + K^{-1} \cdot 2^{-2B/V})$ plus optimization slack, with K nodes, n samples per node, probe set size m , vocabulary size V , and per-node uplink budget B . The first two terms are classical: $d/(Kn)$ is the pooled parametric-MLE rate on Kn effective samples, and $\rho\sqrt{V \log(V/\delta)/m}$ is a Rademacher-type uniform-convergence rate for the aggregator’s softmax-linear fit on m probe contexts, with ρ the Radon–Nikodym ratio that pays for probing under a public marginal Q instead of P_X^* . The bandwidth term $K^{-1} \cdot 2^{-2B/V}$ is the new statistical object: K -fold averaging of independent dithered errors at the aggregator delivers the $1/K$ pickup, the same as in classical distributed estimation under communication constraints [Zhang et al., 2013, Huang and Huo, 2019, Acharya et al., 2020, Garg et al., 2014]. The cited prior work leaves two questions about this piece open: (i) is the rate tight as a matching lower bound, or could a smarter encoder strictly improve? (ii) when uplinks are heterogeneous and node i transmits at most B_i bits, what is the optimal allocation of a fixed aggregate budget $B_{\text{tot}} = \sum_i B_i$? The present paper answers both via a single technical idea, the softmax-Hessian trace bound $\text{tr}(H_{\text{soft}}) \leq 1$ applied to the exact cumulant expansion of softmax-KL, which underpins both the upper bound (Theorem 3.1) and a matching lower bound for the dithered construction (pinning the rate at $\Theta(K^{-1} \cdot 2^{-2B/V})$); the same machinery extends per-node to give a closed-form optimal allocation under heterogeneous budgets with an adaptive plug-in variant.

Contributions.

- 1. Matching lower bound and multi-round achievability (Theorems 4.2 and 4.3).** The dithered FPLD construction has a matching lower bound $\Omega(K^{-1} \cdot 2^{-2B/V})$ under non-degeneracy (Theorem 4.2), pinning the single-round bandwidth-axis rate of the construction at $\Theta(K^{-1} \cdot 2^{-2B/V})$. Sequential refinement with nested/scaled residual quantizers sharpens the achievable rate to $O(K^{-1} \cdot 2^{-2TB/V})$ in T rounds; vanilla FPLD’s bandwidth term is T -independent and is therefore strictly suboptimal for every $T > 1$, identifying a concrete protocol-design improvement available within the same scalar-quantization channel (Theorem 4.3).
- 2. Heterogeneous-bandwidth upper bound and optimal allocation (Theorems 5.4 and 5.5).** The FPLD upper bound generalizes to per-node B_i , with the bandwidth term becoming $(c_3/K^2) \sum_i 2^{-2B_i/V}$. Subject to $\sum_i B_i \leq B_{\text{tot}}$ and

per-node weights w_i , the minimizer is a log-tilted water-filling $B_i^* = B_{\text{tot}}/K + (V/2) \log_2(w_i/\bar{w}_g)$ with \bar{w}_g the geometric mean of the weights.

3. **Adaptive plug-in allocation (Corollary 5.6, Algorithm 2).** A two-stage protocol estimates the weights \hat{w}_i from T_0 warm-up rounds at the uniform pilot allocation and then runs the plug-in water-filling on \hat{w}_i . The resulting allocation is $1 + O(\sqrt{\log(K/\delta)/(mT_0)})$ -suboptimal in the bandwidth term with high probability, requiring no extra channel and no a-priori knowledge of $L_{\ell,i}$.
4. **Numerical illustrations.** On a synthetic n-gram FPLD simulator, empirical expected KL is sandwiched between the upper and lower bounds across both K and B sweeps (Figure 1); the optimal allocation strictly dominates uniform and an inverse-weighted baseline under heterogeneous per-node clip levels (Figure 2).

Scope. This is a focused statistical study of FPLD’s training-time KL rate. Prior work [Dubey and Huo, 2026] develops the full FPLD protocol (recapped as Algorithm 1), the inference-time conformal coverage results (FC-RAG), and the proof of Theorem 3.1. Inference-time coverage, real-LM evaluation, privacy, and Byzantine robustness are out of scope for this paper. The multi-round case is treated as an upper-bound/achievability result for nested/scaled residual quantization (Section 4.1); unrestricted multi-round minimax lower bounds are left open, alongside extension to non-parametric students and a streaming-update variant of Algorithm 2 for non-stationary weights.

2 Setup

Vocabulary, contexts, predictors. Let \mathcal{V} be a finite vocabulary of size V and $\mathcal{X} = \mathcal{V}^{\leq L}$ contexts of length at most L . A predictor is a map $\mathcal{X} \rightarrow \Delta(\mathcal{V})$, where $\Delta(\mathcal{V})$ is the simplex over tokens.

Nodes and data. K nodes; node $i \in \{1, \dots, K\}$ holds an i.i.d. dataset $\mathcal{D}_i = \{(x_j^{(i)}, y_j^{(i)})\}_{j=1}^n$ drawn from P^* on $\mathcal{X} \times \mathcal{V}$. Raw data never leaves a node.

Public probe set. $X_{\text{probe}} = \{x^{(l)}\}_{l=1}^m$, i.i.d. from a probe marginal Q that covers P_X^* in the bounded-Radon–Nikodym sense $\rho = \text{ess sup}_x dP_X^*/dQ < \infty$.

Communication. Bandwidth is charged on uplink only. In the homogeneous case (Section 3), every node transmits at most B bits per probe context per round; in the heterogeneous case (Section 5), node i transmits at most B_i bits. Downlink broadcast of the aggregated student is uncharged, matching standard federated convention.

Estimand. The aggregator produces a global student $\hat{P} : \mathcal{X} \rightarrow \Delta(\mathcal{V})$ approximating P^* ; the risk is $\mathbb{E}_{X \sim P_X^*} [\text{KL}(P^*(\cdot | X) \| \hat{P}(\cdot | X))]$.

3 FPLD Protocol and Upper-Bound Recap

Federated Probe-Logit Distillation (FPLD) replaces gradient or weight exchange with the exchange of *quantized logits on a public probe set*. All nodes initialize from a shared

pretrained base $\hat{P}^{(0)}$. In each of T rounds, a node fine-tunes locally on its private dataset, evaluates its updated model on the probe set, and transmits a per-coordinate scalar-quantized logit vector at B/V bits per coordinate. The aggregator averages the K quantized logit vectors coordinate-wise and distills a global student on the averaged logits, then broadcasts the student back to all nodes. Total uplink is $O(KTmB)$; downlink is uncharged.

Algorithm 1 Federated Probe-Logit Distillation (FPLD).

Require: rounds T ; local epochs E ; per-vector uplink budget B bits; probe set $X_{\text{probe}} = \{x^{(l)}\}_{l=1}^m$; shared base $\hat{P}^{(0)}$.

- 1: **for** $t = 1, \dots, T$ **do**
- 2: **for** each node $i = 1, \dots, K$ **in parallel do**
- 3: $\hat{P}_i^{(t)} \leftarrow \text{FINETUNE}(\hat{P}^{(t-1)}, \mathcal{D}_i, E)$
- 4: **for** $l = 1, \dots, m$ **do**
- 5: $\tilde{\ell}_i^{(t,l)} \leftarrow \text{SCALARQUANTIZE}(\text{LOGITS}(\hat{P}_i^{(t)}, x^{(l)}); B/V \text{ bits/coord}, [-L_\ell, L_\ell])$
- 6: **end for**
- 7: uplink $\{\tilde{\ell}_i^{(t,l)}\}_{l=1}^m$ to aggregator
- 8: **end for**
- 9: $\bar{\ell}^{(t,l)} \leftarrow \frac{1}{K} \sum_i \tilde{\ell}_i^{(t,l)}$ for all l
- 10: $\hat{P}^{(t)} \leftarrow \arg \min_{P \in \mathcal{F}_\Theta} \sum_l \text{KL}(\text{softmax}(\bar{\ell}^{(t,l)}) \| P(\cdot | x^{(l)}))$
- 11: broadcast $\hat{P}^{(t)}$ to all nodes
- 12: **end for**
- 13: **return** $\hat{P} \leftarrow \hat{P}^{(T)}$

We adopt six assumptions on the parametric family (A.2), the probe distribution (A.3), homogeneous data (A.4), local-optimization slack (A.5), the uniform quantization channel (A.6), and the aggregator’s distillation fit (A.7); full statements are in Appendix A.

Theorem 3.1 (FPLD upper bound). *Under assumptions (A.2)–(A.7) and the small-error condition (SE) of Appendix B, there exist absolute constants $c_1, c_2, c_3 > 0$ such that, for every $\delta \in (0, 1)$, with probability at least $1 - \delta$ over the local datasets and the probe draw,*

$$\mathbb{E}_{X \sim P_X^*} \left[\text{KL}(P^*(\cdot | X) \| \hat{P}(\cdot | X)) \right] \leq \frac{c_1 d}{Kn} + c_2 \rho \sqrt{\frac{V \log(V/\delta)}{m}} + \frac{c_3}{K} 2^{-2B/V} + \varepsilon_{\text{opt}} + \varepsilon_{\text{fit}}.$$

Here $c_1 = \Theta(1/\lambda_{\min}(I(\theta^*)))$, c_2 depends only on L_ℓ and the Rademacher constant of softmax-linear classes, and c_3 depends only on L_ℓ and the dithered-quantizer distortion constant C_q ; concretely $c_3 = C_q/2 = L_\ell^2/6$.

Interpretation. The four terms reflect, respectively, pooled parametric-MLE convergence on the Kn effective samples; probe generalization at rate $1/\sqrt{m}$ with a coverage penalty ρ ; exponentially decaying quantization distortion in bits-per-coordinate; and controllable optimization slack. The $1/K$ prefactor of the quantization term comes from averaging K independent dithered errors at the aggregator; the factor of V one might naively expect from summing per-coordinate variances is absorbed by the softmax-Hessian trace bound (Appendix B). The bandwidth term depends on B but not on T : vanilla FPLD does not exploit multi-round refinement to sharpen its quantization rate. Section 4.1 shows this is strictly suboptimal for $T > 1$.

What this paper contributes on top. Theorem 3.1 is the upper-bound half of an analysis already developed in prior work [Dubey and Huo, 2026]. The present paper extends it along two axes: a matching lower bound for the dithered FPLD construction plus a multi-round sequential-refinement achievability result (Section 4, Theorems 4.2 and 4.3); and a heterogeneous-bandwidth generalization with closed-form optimal allocation and an adaptive plug-in variant (Section 5, Theorems 5.4 and 5.5, Corollary 5.6).

4 Matching Lower Bound and Multi-Round Achievability

Given Theorem 3.1’s upper bound at $c_3 K^{-1} \cdot 2^{-2B/V}$, two natural questions follow: (i) is this rate tight as a matching lower bound, and (ii) can it sharpen further across multiple rounds? We answer both within the dithered-FPLD construction. Theorem 4.2 establishes a single-round matching lower bound, pinning the bandwidth-axis rate of the construction at $\Theta(K^{-1} \cdot 2^{-2B/V})$. Theorem 4.3 gives a multi-round achievability rate $O(K^{-1} \cdot 2^{-2TB/V})$ via sequential refinement with nested/scaled residual quantizers; vanilla FPLD’s bandwidth term is T -independent and is therefore strictly suboptimal for every $T > 1$, identifying a concrete protocol-design improvement available within the same scalar-quantization channel.

Protocol class. The single-round FPLD-class protocols $\mathcal{P}_B^{\text{FPLD}}$ consist of those in which each node i observes its local dataset \mathcal{D}_i and the public probe set X_{probe} , applies a per-coordinate clipped scalar quantizer at B/V bits with subtractive dithering (Assumption A.6), and the aggregator forms an unbiased K -fold average. The target class \mathcal{P}^* is the parametric family of conditional distributions P^* for which some $\theta^* \in \text{int}(\Theta)$ realizes $P^* = P_{\theta^*}$ and the per-coordinate logit values lie in $[-L_\ell, L_\ell]$. Both match the operating regime of Theorem 3.1. An unconditional minimax lower bound over the larger class \mathcal{P}_B of arbitrary B -bit-per-node protocols is left open (Section 7).

Theorem 4.2 (Matching lower bound for the dithered FPLD construction). *Under Assumptions A.2–A.7, the non-degeneracy condition*

$$(ND) \quad \mathbb{E}_{X \sim Q} [1 - \|p^*(\cdot | X)\|_2^2] \geq c_p > 0,$$

and the small-error condition (SE’) of Appendix B (a c_p -calibrated variant of (SE); both forms are stated in Appendix B), the bandwidth contribution of the dithered FPLD construction satisfies, for any $K, n, m \geq 1$ and $B \geq V$,

$$\mathbb{E}[\text{KL}(P^* \| \hat{P}_{\text{FPLD}})]_{\text{bandwidth}} \geq \frac{c_p L_\ell^2}{12K} \cdot 2^{-2B/V}.$$

Combined with Theorem 3.1’s upper bound, the bandwidth-axis rate of the dithered FPLD construction is $\Theta(K^{-1} \cdot 2^{-2B/V})$ up to absolute constants: $c_{\text{lb}} = c_p L_\ell^2 / 12$ on the lower-bound side and c_3 on the upper-bound side. The proof, in Appendix B, is a direct computation of the dither variance composed with the softmax-KL cumulant expansion and the trace bound $\text{tr}(H_{\text{soft}}) \leq 1$.

4.1 Multi-round sequential-refinement achievability

Theorem 4.2’s rate is for a single round. Using the bit budget across rounds with nested/scaled residual quantization sharpens the exponent linearly in T .

Multi-round protocol class. Let $\mathcal{P}_{B,T}^{\text{FPLD-ref}}$ denote the class of T -round FPLD-class protocols in which each round transmits B bits per node and each node uses a *nested/scaled residual quantizer*: in round t , the quantizer step size is scaled to the residual range from round $t-1$, equivalently producing an effective (TB/V) -bit scalar quantizer per coordinate after T rounds. A fixed-step residual quantizer that does not rescale across rounds stalls at $O(K^{-1} \cdot 2^{-2B/V})$ regardless of T ; the rescaling is what unlocks the multi-round gain.

Theorem 4.3 (Sequential-refinement achievability). *Under the same assumptions as Theorem 4.2 (with the small-error condition reinterpreted at the effective rate TB/V), sequential refinement achieves*

$$\mathbb{E}[\text{KL}(P^* \parallel \hat{P}_{\text{seq-ref}})]_{\text{bandwidth}} \leq \frac{C'_3}{K} \cdot 2^{-2TB/V} + O\left(\frac{(\log V)^{3/2}}{K^{3/2}} \cdot 2^{-3TB/V}\right),$$

whereas vanilla FPLD stalls at $c_3/K \cdot 2^{-2B/V}$ for every T . The constant C'_3 depends only on the same scalar-quantizer / dither convention as c_3 , coinciding with it under Assumption A.6's dither variance $C_q = L_\ell^2/3$.

The take-away is operational: the T -fold sharpening requires only a change in the per-round residual encoder, not a change in the bit budget or channel structure. Vanilla FPLD as specified in Algorithm 1 does not exploit this; sequential refinement does. The proof iterates the single-round bound on the residual at each round (Appendix B.4).

5 Heterogeneous Bandwidth and Optimal Allocation

The upper bound recapped in Section 3 assumes a uniform per-node bandwidth budget B . Real federated deployments give different nodes different uplinks: hospitals on a metropolitan WAN have one rate; a regional clinic on satellite has another. We drop the uniform- B assumption and let node i transmit at most B_i bits per probe context, then ask how the upper bound generalizes and how a network operator should allocate a fixed aggregate budget $\sum_i B_i \leq B_{\text{tot}}$.

Assumption A.6 (uniform scalar quantization) is replaced by a per-node version.

Assumption 5.1 (Per-node scalar quantization). Each node i clips its per-probe logit vector to $[-L_\ell, L_\ell]^V$ and scalar-quantizes each coordinate to B_i/V bits using a subtractively dithered uniform quantizer. Per-coordinate distortions are bounded: $\mathbb{E}[(\tilde{\ell}_{i,v} - \ell_{i,v})^2] \leq C_q 2^{-2B_i/V}$ with $C_q = L_\ell^2/3$, and quantization errors across nodes and coordinates are independent mean-zero.

Theorem 5.4 (Heterogeneous-bandwidth FPLD upper bound). *Replace Assumption A.6 with Assumption 5.1 and keep Assumptions A.2–A.5 and A.7. Under the small-error condition (**SE**) of Appendix B, there exist absolute constants $c_1, c_2, c_3 > 0$ such that, for every $\delta \in (0, 1)$, with probability at least $1 - \delta$,*

$$\mathbb{E}_X[\text{KL}(P^* \parallel \hat{P})] \leq \frac{c_1 d}{Kn} + c_2 \rho \sqrt{\frac{V \log(V/\delta)}{m}} + \frac{c_3}{K^2} \sum_{i=1}^K 2^{-2B_i/V} + \varepsilon_{\text{opt}} + \varepsilon_{\text{fit}}.$$

The constant $c_1 = \Theta(1/\lambda_{\min}(I(\theta^*)))$ and c_2 are unchanged from the homogeneous case; the bandwidth-term coefficient $c_3 = C_q/2$ is the trace-sharpened constant (no V , no λ_{\min} factor), produced by applying Lemma B.7's trace bound to the per-node aggregated dither covariance in place of the conservative Euclidean-logit $\|\bar{\xi}\|_2^2 = V\sigma^2$ argument. The proof is in Appendix B.5.

Sanity check. If $B_i \equiv B$ for all i , the heterogeneous bandwidth term reduces to $\frac{c_3}{K^2} \cdot K \cdot 2^{-2B/V} = c_3 \frac{1}{K} 2^{-2B/V}$, recovering Theorem 3.1’s sharpened form. The conservative Euclidean route would give $(c'_3 V/K^2) \sum_i 2^{-2B_i/V}$ with $c'_3 = C_q/(2\lambda_{\min}(I(\theta^*)))$, a factor of $V \cdot c'_3/c_3 = V/\lambda_{\min}(I(\theta^*))$ looser than the trace-sharpened form stated here (see App. B.5 for the comparison).

With the upper bound generalized, the natural question is: under a fixed total uplink budget $B_{\text{tot}} = \sum_i B_i$, how should an operator allocate bits across nodes? Theorem 5.5 answers this for the quantization term of Theorem 5.4; the statistical and probe-generalization terms do not depend on the B_i .

Theorem 5.5 (Optimal bandwidth allocation). *Fix per-node weights $w_1, \dots, w_K > 0$ and a total budget $B_{\text{tot}} > 0$. The minimizer of the weighted quantization term*

$$F(B_1, \dots, B_K) = \frac{1}{K^2} \sum_{i=1}^K w_i \cdot 2^{-2B_i/V} \quad \text{subject to} \quad \sum_{i=1}^K B_i = B_{\text{tot}}, \quad B_i \geq 0,$$

is the water-filling allocation

$$B_i^* = \frac{B_{\text{tot}}}{K} + \frac{V}{2} \log_2 \left(\frac{w_i}{\bar{w}_g} \right), \quad \bar{w}_g := \left(\prod_{j=1}^K w_j \right)^{1/K},$$

clipped to $[0, B_{\text{max}}]$ if a per-node cap is imposed (the unclipped formula is applied to the unsaturated subset, with budget redistributed across saturating coordinates). When all w_i are equal, $B_i^ = B_{\text{tot}}/K$.*

Interpretation. The allocation is \log_2 -tilted by the weight ratio: a node with double the weight gets $V/2$ extra bits. Because the weight w_i in our setting tracks per-node logit variance, the allocation gives more bits to noisier nodes. This is the same direction as classical reverse-water-filling for distortion-rate optimization, applied per-node rather than per-source.

What the weights w_i should be. Theorem 5.5 treats w_i as given. The natural choice in our setting is the per-node contribution to the quantization-term constant of Theorem 5.4. Under Assumption 5.1’s uniform clip L_ℓ , every node has $w_i = 1$ and the optimal allocation is uniform. If clipping levels differ across nodes (e.g., a node with calibrated logit range $L_{\ell,i}$), then $w_i \propto L_{\ell,i}^2$ and the bit allocation tilts proportionally. We use this clip-variance formulation in the experiments (Section 6). The proof of Theorem 5.5 is one Lagrangian (Appendix B.6).

5.1 Adaptive bandwidth allocation

Theorem 5.5 treats the per-node weights w_i as inputs. In practice, an operator rarely knows them in advance: per-node clip levels and logit-magnitude profiles vary across deployments and across rounds. We close this gap with a two-stage protocol that estimates w_i from warm-up-round quantized probe logits and then applies the plug-in water-filling allocation. The construction requires no extra channel and no a-priori knowledge of $L_{\ell,i}$.

Estimator. Run the protocol for $T_0 \geq 1$ warm-up rounds at the uniform pilot allocation $B_i = B_{\text{tot}}/K$. The aggregator records the received quantized probe logits $\tilde{\ell}_{i,v}^{(l,t)}$ and forms

$$\hat{w}_i = \frac{1}{T_0 m V} \sum_{t=1}^{T_0} \sum_{l=1}^m \sum_{v=1}^V (\tilde{\ell}_{i,v}^{(l,t)})^2, \quad w_i := \mathbb{E} \left[\frac{1}{V} \|\tilde{\ell}_i\|_2^2 \right].$$

This estimates the population per-node second moment w_i (the quantity tracked by “weight \propto logit variance” in the discussion after Theorem 5.5) entirely from data the aggregator already receives under Assumption 5.1.

Corollary 5.6 (Adaptive bandwidth allocation). *Let $\hat{B}_i^* = B_{\text{tot}}/K + (V/2) \log_2(\hat{w}_i/\hat{w}_g)$ with $\hat{w}_g = (\prod_j \hat{w}_j)^{1/K}$ be the plug-in water-filling allocation computed from the warm-up estimator. Under Assumption 5.1 and $w_{\min} := \min_i w_i > 0$, for every $\delta \in (0, 1)$, with probability at least $1 - \delta$,*

$$F(\hat{B}^*) \leq \left(1 + c_{\text{ad}} \sqrt{\log(K/\delta)/(m T_0)} \right) F(B^*),$$

where c_{ad} depends only on the clip cap L_ℓ and on w_{\min} . The cost of adaptivity vanishes at rate $1/\sqrt{m T_0}$ in the warm-up sample size; in particular, one warm-up round and a probe set of size $m \gtrsim \log(K/\delta)/\eta^2$ suffice for relative suboptimality at most η .

Proof sketch. (i) *Relative-error transfer.* Direct substitution of \hat{B}_i^* into the per-node objective gives $F(\hat{B}^*)/F(B^*) = K^{-1} \sum_i (w_i/\hat{w}_i)(\hat{w}_g/\bar{w}_g) \leq 1 + 2\eta + 4\eta^2$ when $|\hat{w}_i - w_i| \leq \eta w_i$ holds uniformly in i (full derivation in Lemma B.8). (ii) *Concentration.* Let $S_{i,t,l} := \frac{1}{V} \sum_v (\tilde{\ell}_{i,v}^{(l,t)})^2$ be the per-context block average for node i at round t and probe l , taking values in $[0, R_\ell^2]$ with post-quantization range $R_\ell := L_\ell(1 + 2^{-B_{\text{tot}}/(KV)}) \leq 2L_\ell$ (this R_ℓ absorbs the subtractively dithered quantizer’s worst-case overshoot beyond the input clip). The $\{S_{i,t,l}\}$ are i.i.d. across (t, l) for each fixed i by Assumption 5.1 and the i.i.d. probe draw, so Hoeffding plus a K -fold union bound gives $|\hat{w}_i - w_i| \leq R_\ell^2 \sqrt{\log(2K/\delta)/(2m T_0)}$ uniformly. Composing (i) and (ii) yields the claim; the full proof is in Appendix B.7.

6 Numerical Illustrations

We test Theorems 3.1, 4.2, 5.4, and 5.5 on a synthetic n-gram FPLD simulator. Each node observes a noisy logit estimate of a fixed common P^* over $V = 256$ tokens (estimation noise variance $1/n$ per coordinate, $n = 30,000$), and transmits scalar-quantized logits at B/V (or B_i/V) bits per coordinate via a subtractively dithered uniform quantizer. The aggregator averages quantized logits coordinate-wise and emits the softmax student. Empirical KL is reported across 30 seeds per point for Figure 1 and 100 for Figure 2; both use a single fixed P^* so per-axis variability isolates the bandwidth effect. The simulator is a controlled sandbox designed to verify the predicted rate shapes ($1/K$ shrinkage, $2^{-2B/V}$ decay, water-filling dominance) on a setting where the dithered-quantization channel is exact; end-to-end evaluation on real language-model training is out of scope (§ 1).

Bound bracketing (Figure 1). Empirical FPLD KL is bracketed by Theorem 3.1’s upper bound and Theorem 4.2’s matching lower bound, both at the $K^{-1} \cdot 2^{-2B/V}$ rate: the K -sweep at $B/V = 4$ shows the predicted $1/K$ shrinkage, and the B -sweep at $K = 4$ shows

Algorithm 2 Adaptive FPLD with two-stage bandwidth allocation.

Require: K nodes; total budget B_{tot} ; probe set X_{probe} of size m ; warm-up rounds $T_0 \geq 1$; total rounds $T \geq T_0 + 1$; per-node cap $B_{\text{max}} \geq B_{\text{tot}}/K$.

Stage A: warm-up at uniform pilot allocation.

- 1: **for** $t = 1, \dots, T_0$ **do**
 - 2: **for** each node $i = 1, \dots, K$ **in parallel do**
 - 3: transmit B_{tot}/K bits per probe context to aggregator
 - 4: **end for**
 - 5: aggregator records $\tilde{\ell}_{i,v}^{(l,t)}$ for all (i, l, v)
 - 6: **end for**
 - 7: $\hat{w}_i \leftarrow (T_0 m V)^{-1} \sum_{t,l,v} (\tilde{\ell}_{i,v}^{(l,t)})^2$ for each i
 - Stage B: refinement at plug-in allocation.**
 - 8: $\hat{w}_g \leftarrow (\prod_{j=1}^K \hat{w}_j)^{1/K}$
 - 9: $\hat{B}_i \leftarrow \text{clip}(B_{\text{tot}}/K + (V/2) \log_2(\hat{w}_i/\hat{w}_g), 0, B_{\text{max}})$ for each i
 - 10: **if** any \hat{B}_i is saturated at B_{max} **then**
 - 11: redistribute residual budget across the unsaturated subset by re-solving Theorem 5.5 on that subset
 - 12: **end if**
 - 13: **for** $t = T_0 + 1, \dots, T$ **do**
 - 14: **for** each node i **in parallel do**
 - 15: transmit \hat{B}_i bits per probe context
 - 16: **end for**
 - 17: **end for**
 - 18: aggregator runs the FPLD aggregation rule on all received logits and emits the final student \hat{P}
-

the predicted exponential decay in B/V (KL roughly quartering with each additional bit per coordinate). The bracketing is the qualitative claim; the specific multiplicative constants c_3 and c_{lb} are illustrative.

Allocation policy (Figure 2). With $K = 4$ nodes and heterogeneous per-node clip levels $L = (1, 1, 4, 4)$ (weights $w_i = L_i^2 = (1, 1, 16, 16)$), mirroring the running example with two metropolitan-WAN hospitals at wider uplink paired with two satellite clinics at narrower uplink), the optimal allocation (Theorem 5.5) strictly dominates uniform at every aggregate budget where bandwidth matters: at $B_{\text{tot}}/V = 8$ the optimal achieves $\text{KL} \approx 1.1 \times 10^{-2}$, roughly half of uniform’s 2.3×10^{-2} , and the gap persists at higher budgets. Inverse-weighted plateaus at $\approx 8 \times 10^{-2}$ across the full range (roughly an order of magnitude above the optimal), validating that the qualitative direction of Theorem 5.5 (more bits to higher-variance nodes) is correct.

7 Discussion

Position vs distributed estimation. Theorems 4.2 and 4.3 parallel the classical lower-bound and achievability program for communication-constrained distributed estimation [Zhang et al., 2013, Huang and Huo, 2019, Acharya et al., 2020, Garg et al., 2014], specialized here to the per-coordinate scalar-quantization channel on logit vec-

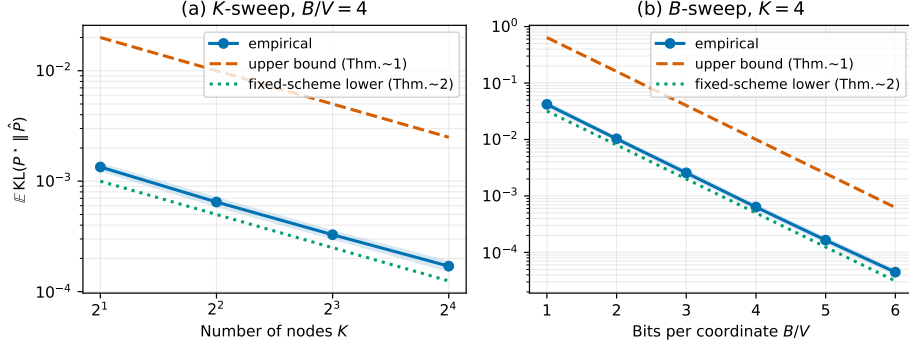


Figure 1: Empirical FPLD KL (solid blue) bracketed by Theorem 3.1’s upper bound (dashed orange) and Theorem 4.2’s matching lower bound (dotted teal). Synthetic n -gram simulator, $V = 256$, $n = 30,000$, 30 seeds per point. The K -sweep at $B/V = 4$ shows $1/K$ shrinkage; the B -sweep at $K = 4$ shows exponential decay in B/V . Constants are illustrative.

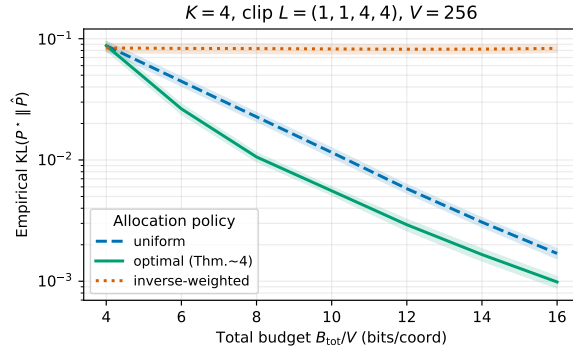


Figure 2: Heterogeneous bandwidth allocation: optimal (solid teal), uniform (dashed blue), and inverse-weighted (dotted orange), $K = 4$ nodes with per-node clip levels $L = (1, 1, 4, 4)$. Optimal dominates uniform by roughly $2\times$ at $B_{\text{tot}}/V = 8$ and the gap persists at higher budgets; inverse-weighted plateaus near 8×10^{-2} . 100 seeds per point.

tors over a shared probe set. The technique differs: we apply the softmax-Hessian trace bound to the exact cumulant expansion under independent mean-zero dithering. Our sequential-refinement achievability improves the bandwidth-axis rate linearly in T within the FPLD-class scheme; an unconditional minimax lower bound over arbitrary B -bit-per-node protocols remains open.

Position vs federated distillation. FedFD [Li et al., 2025] and FedDF [Lin et al., 2020] demonstrate federated distillation in practice but prove no rate; our heterogeneous-bandwidth result (Theorem 5.4) closes that gap and pairs it with a closed-form allocation rule.

References

- Jayadev Acharya, Clément L. Canonne, and Himanshu Tyagi. Inference under information constraints i: Lower bounds from chi-square contraction. *IEEE Transactions on Information Theory*, 66(12):7835–7855, 2020. doi: 10.1109/TIT.2020.3028440.
- Prasanjit Dubey and Xiaoming Huo. Federated language models under bandwidth budgets: Distillation rates and conformal coverage, 2026. URL <https://arxiv.org/abs/2605.09986>.
- Ankit Garg, Tengyu Ma, and Huy L. Nguyễn. On communication cost of distributed statistical estimation and dimensionality. In Z. Ghahramani, M. Welling, C. Cortes, N. Lawrence, and K. Weinberger, editors, *Advances in Neural Information Processing Systems*, volume 27. Curran Associates, Inc., 2014. URL https://proceedings.neurips.cc/paper_files/paper/2014/file/29883d52f2590df7dfb27c69493c91d8-Paper.pdf.
- Cheng Huang and Xiaoming Huo. A distributed one-step estimator. *Mathematical Programming*, 174(1–2):41–76, 2019. doi: 10.1007/s10107-019-01369-0.
- Yichen Li, Xiuying Wang, Wenchao Xu, Haozhao Wang, Yining Qi, Jiahua Dong, and Ruixuan Li. Feature distillation is the better choice for model-heterogeneous federated learning. In D. Belgrave, C. Zhang, H. Lin, R. Pascanu, P. Koniusz, M. Ghassemi, and N. Chen, editors, *Advances in Neural Information Processing Systems*, volume 38, pages 104726–104744. Curran Associates, Inc., 2025. URL https://proceedings.neurips.cc/paper_files/paper/2025/file/96dd63ab8fd79163a5399e0b385f208d-Paper-Conference.pdf.
- Tao Lin, Lingjing Kong, Sebastian U Stich, and Martin Jaggi. Ensemble distillation for robust model fusion in federated learning. In H. Larochelle, M. Ranzato, R. Hadsell, M.F. Balcan, and H. Lin, editors, *Advances in Neural Information Processing Systems*, volume 33, pages 2351–2363. Curran Associates, Inc., 2020. URL https://proceedings.neurips.cc/paper_files/paper/2020/file/18df51b97ccd68128e994804f3eccc87-Paper.pdf.
- Yuchen Zhang, John C. Duchi, and Martin J. Wainwright. Communication-efficient algorithms for statistical optimization. *Journal of Machine Learning Research*, 14(104):3321–3363, 2013. URL <http://jmlr.org/papers/v14/zhang13b.html>.

Supplementary Material

A Assumption block

Assumption A.2 (Parametric well-specification). $P^* \in \mathcal{F}_\Theta = \{P_\theta : \theta \in \Theta\}$ with $\Theta \subset \mathbb{R}^d$ compact, $\theta^* \in \text{int}(\Theta)$ exists with $P_{\theta^*} = P^*$, and the Fisher information $I(\theta^*) \succ 0$ is positive definite. Standard smoothness holds (twice continuous differentiability of $\log p_\theta$).

Assumption A.3 (Probe coverage). Q covers P_X^* with bounded Radon–Nikodym derivative $\rho = \text{ess sup}_x dP_X^*/dQ < \infty$.

Assumption A.4 (Homogeneous data). $P_i = P^*$ for all nodes i .

Assumption A.5 (Local optimization slack). Every local optimizer terminates within mean-squared distance ε_{opt} of the local MLE: $\mathbb{E}\|\hat{\theta}_i^{(t)} - \hat{\theta}_i^{\text{MLE}}\|^2 \leq \varepsilon_{\text{opt}}$.

Assumption A.6 (Uniform scalar quantization). Each node clips its per-probe logit vector to $[-L_\ell, L_\ell]^V$ and scalar-quantizes each coordinate to B/V bits using a subtractively dithered uniform quantizer; per-coordinate distortion satisfies $\mathbb{E}[(\tilde{\ell}_v - \ell_v)^2] \leq C_q 2^{-2B/V}$ with $C_q = L_\ell^2/3$, errors independent across nodes and coordinates.

Assumption A.7 (Distillation fit). The aggregator’s distillation step produces $\hat{P} \in \mathcal{F}_\Theta$ within ε_{fit} of the infimum of empirical probe-KL.

B Proofs

This appendix collects the proofs deferred from the main text. § B.1 states the softmax-Hessian trace bound used throughout. § B.2 derives the bandwidth-term form of Theorem 3.1 via the trace bound (paralleling the analogous derivation in the companion paper [Dubey and Huo, 2026]). The remaining subsections follow the order of the corresponding statements in the body: § B.3 proves the matching lower bound of Theorem 4.2; § B.4 proves the sequential-refinement achievability of Theorem 4.3; § B.5 proves the heterogeneous-bandwidth upper bound of Theorem 5.4; § B.6 proves the optimal-allocation closed form of Theorem 5.5; § B.7 proves the adaptive-allocation Corollary 5.6.

B.1 Softmax-Hessian trace bound

Lemma B.7 (Softmax Hessian trace bound). *For any $p \in \Delta(\mathcal{V})$:*

$$\begin{aligned}
 H_{\text{soft}}(p) &= \text{diag}(p) - pp^\top && \text{[categorical softmax Fisher/Hessian]} \\
 \text{tr}(H_{\text{soft}}(p)) &= \text{tr}(\text{diag}(p)) - \text{tr}(pp^\top) && \text{[linearity of trace]} \\
 &= \sum_v p_v - \sum_v p_v^2 && \text{[trace of diagonal and rank-one matrices]} \\
 &= 1 - \|p\|_2^2 && \text{[}\sum_v p_v = 1\text{]} \\
 &\leq 1 && \text{[}\|p\|_2^2 \geq 0\text{]}
 \end{aligned}$$

So $\text{Cov}(\bar{\varepsilon}) \preceq \sigma^2 I_V$ with $\sigma^2 := C_q \cdot 2^{-2B/V} / K$.

Apply the trace bound:

$$\begin{aligned} \text{tr}(H_{\text{soft}}(p^*) \cdot \text{Cov}(\bar{\varepsilon})) &\leq \sigma^2 \cdot \text{tr}(H_{\text{soft}}(p^*)) \quad \left[\begin{array}{l} \text{tr}(AB) \leq \text{tr}(A) \cdot \|B\|_{\text{op}} \text{ for } \\ A \succeq 0; \|\text{Cov}(\bar{\varepsilon})\|_{\text{op}} \leq \sigma^2 \end{array} \right] \\ &\leq \sigma^2 \quad \text{[Lemma B.7: } \text{tr}(H_{\text{soft}}) \leq 1] \end{aligned}$$

Bound the cubic remainder:

$$\begin{aligned} \mathbb{E}\|\bar{\varepsilon}\|_{\infty}^3 &\leq C' \sigma^3 (\log V)^{3/2} \quad \text{[maximum of } V \text{ sub-Gaussians; standard tail bound]} \\ |\mathbb{E}[\kappa_3(\bar{\varepsilon})]| &\leq C \cdot C' \sigma^3 (\log V)^{3/2} \quad \text{[cubic remainder absolute bound]} \\ &= C'' \cdot \frac{(\log V)^{3/2}}{K^{3/2}} \cdot 2^{-3B/V} \quad \left[\sigma = \sqrt{C_q/K} \cdot 2^{-B/V} \right] \end{aligned}$$

Combine:

$$\begin{aligned} \mathbb{E}_{\bar{\varepsilon}}[\text{KL}] &= \frac{1}{2} \text{tr}(H_{\text{soft}}(p^*) \cdot \text{Cov}(\bar{\varepsilon})) + \mathbb{E}[\kappa_3(\bar{\varepsilon})] \quad \text{[from the expectation chain above]} \\ &\leq \frac{1}{2} \sigma^2 + C'' \frac{(\log V)^{3/2}}{K^{3/2}} \cdot 2^{-3B/V} \quad \text{[trace bound + cubic remainder bound]} \\ &= \frac{C_q}{2K} \cdot 2^{-2B/V} + O\left(\frac{(\log V)^{3/2}}{K^{3/2}} \cdot 2^{-3B/V}\right) \quad \text{[substitute } \sigma^2 = C_q \cdot 2^{-2B/V} / K] \end{aligned}$$

Setting $c_3 = C_q/2$ recovers the theorem statement under (SE). The V -factor cancellation arises directly from $\text{tr}(H_{\text{soft}}) \leq 1$ in the second step of the trace bound; in contrast, the conservative Euclidean-logit bound uses $\mathbb{E}\|\bar{\varepsilon}\|_2^2 = V\sigma^2$ and the operator norm $\|H_{\text{soft}}\|_{\text{op}} \leq 1/2$, which produces the V/K form. \square

B.3 Proof of Theorem 4.2

We prove Theorem 4.2: under Assumptions A.2–A.7 together with (ND) and **(SE')** $2^{-B/V} (\log V)^{3/2} / \sqrt{K} \leq c_0(c_p, L_\ell, C)$ where c_0 is chosen so $C \cdot \sigma (\log V)^{3/2} \leq c_p/4$, the bandwidth contribution of the dithered FPLD construction satisfies $\mathbb{E}[\text{KL}(P^* \parallel \hat{P}_{\text{FPLD}})]_{\text{bandwidth}} \geq c_p L_\ell^2 / (12K) \cdot 2^{-2B/V}$.

Proof. Compute the dither variance directly under Assumption A.6. The uniform quantizer on $[-L_\ell, L_\ell]$ at B/V bits has step size

$$\begin{aligned} \Delta &= \frac{2L_\ell}{2^{B/V}} = 2L_\ell \cdot 2^{-B/V} \quad \text{[uniform partition of } [-L_\ell, L_\ell] \text{ into } 2^{B/V} \text{ cells]} \\ \varepsilon_{i,v} &\sim \text{Unif}[-\Delta/2, +\Delta/2] \quad \text{[subtractive dither, no overload by Assumption A.6]} \\ \mathbb{E}[\varepsilon_{i,v} \mid X] &= 0 \quad \text{[subtractive dither is unbiased]} \\ \text{Var}(\varepsilon_{i,v} \mid X) &= \frac{\Delta^2}{12} \quad \text{[variance of uniform on an interval of length } \Delta] \\ &= \frac{(2L_\ell)^2 \cdot 2^{-2B/V}}{12} \quad \text{[substitute } \Delta = 2L_\ell \cdot 2^{-B/V}] \\ &= \frac{L_\ell^2}{3} \cdot 2^{-2B/V} \quad \text{[simplify]} \end{aligned}$$

The aggregator forms $\bar{\varepsilon}_v = (1/K) \sum_{i=1}^K \varepsilon_{i,v}$. Conditional on X :

$$\begin{aligned} \mathbb{E}[\bar{\varepsilon}_v | X] &= 0 && \text{[linearity; each } \varepsilon_{i,v} \text{ is conditionally mean-zero]} \\ \text{Var}(\bar{\varepsilon}_v | X) &= \frac{1}{K^2} \sum_{i=1}^K \text{Var}(\varepsilon_{i,v} | X) && \text{[independence across nodes; no cross terms]} \\ &= \frac{1}{K^2} \cdot K \cdot \frac{L_\ell^2}{3} \cdot 2^{-2B/V} && \text{[substitute per-node variance]} \\ &= \frac{L_\ell^2}{3K} \cdot 2^{-2B/V} && \text{[simplify]} \\ \text{Cov}(\bar{\varepsilon} | X) &= \sigma^2 I_V, \quad \sigma^2 := \frac{L_\ell^2}{3K} \cdot 2^{-2B/V} && \text{[independence across coordinates by Assumption A.6]} \end{aligned}$$

Apply the exact softmax-KL cumulant expansion conditional on X :

$$\begin{aligned} \mathbb{E}_\varepsilon[\text{KL}(\text{softmax}(\ell^*(X)) \parallel \text{softmax}(\ell^*(X) + \bar{\varepsilon})) | X] &= \frac{1}{2} \text{tr}(H_{\text{soft}}(p^*(\cdot | X)) \cdot \text{Cov}(\bar{\varepsilon} | X)) + R_3(X) && \text{[cumulant expansion; } R_3 \text{ is the cubic remainder]} \\ &= \frac{\sigma^2}{2} \text{tr}(H_{\text{soft}}(p^*(\cdot | X))) + R_3(X) && \text{[Cov}(\bar{\varepsilon} | X) = \sigma^2 I_V \text{]} \end{aligned}$$

Take expectation over $X \sim Q$:

$$\begin{aligned} \mathbb{E}_{X, \bar{\varepsilon}}[\text{KL}] &= \frac{\sigma^2}{2} \mathbb{E}_X[\text{tr}(H_{\text{soft}}(p^*(\cdot | X)))] + \mathbb{E}_X[R_3(X)] && \text{[linearity]} \\ &= \frac{\sigma^2}{2} \mathbb{E}_X[1 - \|p^*(\cdot | X)\|_2^2] + \mathbb{E}_X[R_3(X)] && \text{[tr}(H_{\text{soft}}(p)) = 1 - \|p\|_2^2 \text{ by Lemma B.7]} \\ &\geq \frac{\sigma^2 c_p}{2} - |\mathbb{E}_X[R_3(X)]| && \text{[apply (ND); bound the remainder in absolute value]} \end{aligned}$$

Apply (SE') to dominate the cubic remainder. The remainder satisfies $|\mathbb{E}_X[R_3(X)]| \leq C\sigma^3(\log V)^{3/2}$; under (SE'), $c_0(c_p, L_\ell, C)$ is chosen so $C \cdot \sigma \cdot (\log V)^{3/2} \leq c_p/4$, equivalently $|\mathbb{E}_X[R_3(X)]| \leq (c_p/4) \cdot \sigma^2$. Hence:

$$\begin{aligned} \mathbb{E}_{X, \bar{\varepsilon}}[\text{KL}] &\geq \frac{\sigma^2 c_p}{2} - \frac{c_p \sigma^2}{4} && \text{[cubic remainder bounded by (SE')]} \\ &= \frac{c_p \sigma^2}{4} && \text{[combine]} \\ &= \frac{c_p}{4} \cdot \frac{L_\ell^2}{3K} \cdot 2^{-2B/V} && \text{[substitute } \sigma^2 = L_\ell^2/(3K) \cdot 2^{-2B/V} \text{]} \\ &= \frac{c_p L_\ell^2}{12K} \cdot 2^{-2B/V} && \text{[simplify to closed form]} \end{aligned}$$

This is the displayed lower bound with $c_{\text{lb}} := c_p L_\ell^2/12$. □

Remark on scope. Theorem 4.2 is a lower bound for the subtractively dithered FPLD construction (Assumption A.6); the unconditional minimax bandwidth-axis lower bound over the larger class \mathcal{P}_B of arbitrary B -bit-per-node protocols (alternative quantizers such as biased, vector, learned-codebook, or adaptive ones lie outside Assumption A.6) remains open (see § 7).

B.4 Proof of Theorem 4.3

Theorem 4.3 is an achievability statement: sequential refinement with nested/scaled residual quantizers and B bits per round per node achieves $O(K^{-1} \cdot 2^{-2TB/V})$. The proof iterates the single-round trace-sharpened upper bound of Theorem 3.1 over the residual at each round.

Setup. In round $t \in \{1, \dots, T\}$, each node i holds the residual $r^{(t-1)}(X) := \ell^*(X) - \hat{\ell}^{(t-1)}(X)$, where $\hat{\ell}^{(0)}(X) = 0$ (or any common initialization) and $\hat{\ell}^{(t-1)}(X) = (1/K) \sum_i \tilde{r}_i^{(t-1)}(X)$ is the aggregator's broadcast after round $t - 1$. The nested/scaled quantizer of round t uses step size

$$\begin{aligned} \Delta_t &= 2L_\ell^{(t)} \cdot 2^{-B/V} && \text{[rescaled to round-}t \text{ residual range]} \\ L_\ell^{(t)} &\asymp L_\ell \cdot 2^{-(t-1)B/V} && \text{[residual range after } t-1 \text{ rounds of refinement]} \end{aligned}$$

The post-aggregation residual variance per coordinate, $\sigma_t^2 := \text{Var}(\hat{\ell}_v^{(t)} - \ell_v^* \mid X)$, satisfies a geometric recursion:

$$\begin{aligned} \sigma_t^2 &\asymp \frac{\Delta_t^2}{12K} && \left[\begin{array}{l} \text{trace-sharpened upper} \\ \text{bound applied to round-}t \\ \text{residual, } K\text{-fold averaged} \end{array} \right] \\ &= \frac{(L_\ell^{(t)})^2}{3K} \cdot 2^{-2B/V} && \text{[substitute } \Delta_t = 2L_\ell^{(t)} \cdot 2^{-B/V}] \\ &\asymp \frac{L_\ell^2 \cdot 2^{-2(t-1)B/V}}{3K} \cdot 2^{-2B/V} && \text{[substitute } L_\ell^{(t)} \asymp L_\ell \cdot 2^{-(t-1)B/V}] \\ &= \frac{L_\ell^2}{3K} \cdot 2^{-2tB/V} && \text{[combine exponents]} \end{aligned}$$

After T rounds, $\sigma_T^2 \asymp L_\ell^2/(3K) \cdot 2^{-2TB/V}$. Applying the trace bound from Lemma B.7 to the final aggregated residual:

$$\begin{aligned} \mathbb{E}[\text{KL}(P^* \parallel \hat{P}_{\text{seq-ref}})]_{\text{bandwidth}} &\leq \frac{1}{2} \sigma_T^2 \cdot \text{tr}(H_{\text{soft}}) + \text{cubic remainder} && \left[\begin{array}{l} \text{Trace-sharpened cumulant} \\ \text{chain (§ B.2) applied at} \\ \text{round } T \end{array} \right] \\ &\leq \frac{1}{2} \sigma_T^2 + O(\sigma_T^3 (\log V)^{3/2}) && \left[\text{tr}(H_{\text{soft}}) \leq 1 \right] \\ &= \frac{C'_3}{K} \cdot 2^{-2TB/V} + O\left(\frac{(\log V)^{3/2}}{K^{3/2}} \cdot 2^{-3TB/V}\right) && \left[\begin{array}{l} \text{substitute} \\ \sigma_T^2 = L_\ell^2/(3K) \cdot 2^{-2TB/V}; \text{ set} \\ C'_3 := L_\ell^2/6 \end{array} \right] \end{aligned}$$

Here C'_3 is a possibly different constant from Theorem 3.1's c_3 , depending only on the same scalar-quantizer / dither convention (the two coincide when $C_q = L_\ell^2/3$, the standard subtractive-uniform dither variance under Assumption A.6, in which case $C'_3 = c_3$). The vanilla FPLD comparison is the special case where each round re-quantizes the full ℓ^* at full range L_ℓ (rather than the shrinking residual), so σ_t^2 does not decrease across rounds and the bandwidth term stalls at $L_\ell^2/(6K) \cdot 2^{-2B/V}$ for every T . \square

Note on protocol class. The above proof relies on each round being an FPLD-class protocol on the residual, with the quantizer step rescaled to the residual range. A matching

unconditional multi-round minimax lower bound over arbitrary B -bit interactive protocols is not claimed. Within the same scalar-refinement FPLD multi-round class under (ND) and (SE'), Theorem 4.2's dither-variance chain applied at round T gives a fixed-scheme lower bound $\Omega(K^{-1} \cdot 2^{-2TB/V})$.

B.5 Proof of Theorem 5.4

The aggregator's averaged quantized logits are $\bar{\ell}(x) = \frac{1}{K} \sum_i \tilde{\ell}_i(x)$ where $\tilde{\ell}_i = \ell_i + \xi_i$, with ℓ_i the empirical logit produced by node i 's local optimizer and ξ_i the dithered quantization noise (zero-mean and independent across nodes/coordinates, Assumption 5.1). The student \hat{P} fits the soft-max of $\bar{\ell}$ within ε_{fit} (Assumption A.7), and local optimizers terminate within ε_{opt} of the local MLE (Assumption A.5).

The proof follows the same structure as the homogeneous-bandwidth case (Theorem 3.1; full derivation in the companion paper [Dubey and Huo, 2026]), with the sole modification being that the per-node budgets B_i replace the uniform B in the bandwidth term. The data, probe-generalization, and distillation-fit terms are inherited unchanged from that derivation. We record below the only step that changes: the cumulant-trace bound on the bandwidth contribution.

Cumulant-trace decomposition. Write $\bar{\ell} - \ell^* = (\bar{\ell}^{\text{emp}} - \ell^*) + \bar{\xi}$, with $\bar{\ell}^{\text{emp}} = \frac{1}{K} \sum_i \ell_i$ the average of node logits before quantization and $\bar{\xi} = \frac{1}{K} \sum_i \xi_i$ the averaged dither. By Assumption 5.1, $\bar{\xi}$ is independent of $\bar{\ell}^{\text{emp}} - \ell^*$ and has zero mean. Expanding the softmax-KL via the exact cumulant identity of § B.2 and taking expectations,

$$\mathbb{E}[\text{KL}(P^* \parallel \hat{P})] = \frac{1}{2} \text{tr}(H_{\text{soft}}(p^*) \cdot \text{Cov}(\bar{\ell} - \ell^*)) + \varepsilon_{\text{opt}} + \varepsilon_{\text{fit}} + O\left(\frac{(\log V)^{3/2}}{K^{3/2}}\right).$$

By independence and zero-mean of $\bar{\xi}$, cross-cumulants vanish at second order and the covariance splits additively: $\text{Cov}(\bar{\ell} - \ell^*) = \text{Cov}(\bar{\ell}^{\text{emp}} - \ell^*) + \text{Cov}(\bar{\xi})$. The trace pulls through, separating the KL bound into a data-fluctuation contribution and a bandwidth contribution.

Term (I): data and probe contributions. $\frac{1}{2} \text{tr}(H_{\text{soft}}(p^*) \cdot \text{Cov}(\bar{\ell}^{\text{emp}} - \ell^*))$ is the same data-fluctuation contribution that appears in the homogeneous case. It is bounded by $c_1 d/(Kn)$ (pooled parametric-MLE convergence on Kn effective samples plus the local quadratic expansion of KL at θ^*) and $c_2 \rho \sqrt{V} \log(V/\delta)/m$ (Rademacher uniform convergence of the softmax-linear class over the m probe contexts), exactly as in the homogeneous case; the per-node B_i do not enter this term.

Term (II): bandwidth. Under Assumption 5.1's coordinate-wise independence, $\text{Cov}(\bar{\xi})$ is diagonal with v -th entry $(1/K^2) \sum_{i=1}^K \text{Var}(\xi_{i,v}) \leq (1/K^2) \sum_i C_q 2^{-2B_i/V}$. Hence $\text{Cov}(\bar{\xi}) \preceq \sigma^2 I_V$ with

$$\sigma^2 := \frac{1}{K^2} \sum_{i=1}^K C_q 2^{-2B_i/V}.$$

Applying Lemma B.7's trace bound $\text{tr}(H_{\text{soft}}) \leq 1$ together with the standard inequality $\text{tr}(AB) \leq \|B\|_{\text{op}} \text{tr}(A)$ for $A \succeq 0$,

$$\frac{1}{2} \text{tr}(H_{\text{soft}}(p^*) \cdot \text{Cov}(\bar{\xi})) \leq \frac{\sigma^2}{2} = \frac{C_q}{2K^2} \sum_{i=1}^K 2^{-2B_i/V}.$$

Setting $c_3 = C_q/2$ recovers the bandwidth term $(c_3/K^2) \sum_i 2^{-2B_i/V}$ stated in Theorem 5.4. The cubic remainder is dominated under (SE) by the same argument as in § B.2.

Combining Term (I), Term (II), and the slack terms yields the bound stated in Theorem 5.4. \square

Remark (heterogeneous clip levels). The argument extends directly to per-node clip levels $L_{\ell,i}$ (replacing the uniform L_ℓ in Assumption 5.1). With per-node dither variance bound $C_{q,i} = L_{\ell,i}^2/3$, the bandwidth term takes the form $(1/(2K^2)) \sum_i C_{q,i} \cdot 2^{-2B_i/V} = (1/(6K^2)) \sum_i L_{\ell,i}^2 \cdot 2^{-2B_i/V}$. This fits Theorem 5.5's objective $(1/K^2) \sum_i w_i \cdot 2^{-2B_i/V}$ with $w_i = L_{\ell,i}^2$ (an overall constant drops out of the water-filling formula, since it depends on w_i only through the ratio w_i/\bar{w}_g). This is the form tested in Figure 2 with per-node clips $L_i = (1, 1, 4, 4)$.

B.6 Proof of Theorem 5.5

The objective F is convex in each B_i : it is the sum of decaying exponentials in a positive linear function of B_i , weighted by $w_i > 0$. The constraint set is a simplex slice $\{B \in \mathbb{R}_{\geq 0}^K : \sum_i B_i = B_{\text{tot}}\}$, which is convex. Form the Lagrangian

$$\mathcal{L}(B, \lambda) = \frac{1}{K^2} \sum_{i=1}^K w_i 2^{-2B_i/V} + \lambda \left(\sum_{i=1}^K B_i - B_{\text{tot}} \right).$$

Stationarity, $\partial \mathcal{L} / \partial B_i = 0$, gives

$$-\frac{2 \ln 2}{VK^2} w_i \cdot 2^{-2B_i/V} + \lambda = 0 \iff 2^{-2B_i/V} = \frac{\lambda VK^2}{2w_i \ln 2}.$$

Taking \log_2 ,

$$B_i = -\frac{V}{2} \log_2 \left(\frac{\lambda VK^2}{2w_i \ln 2} \right) = \frac{V}{2} \log_2(w_i) + \text{const}(\lambda).$$

Imposing $\sum_i B_i = B_{\text{tot}}$ pins down the constant:

$$B_i^* = \frac{B_{\text{tot}}}{K} + \frac{V}{2} \log_2(w_i) - \frac{V}{2K} \sum_{j=1}^K \log_2(w_j) = \frac{B_{\text{tot}}}{K} + \frac{V}{2} \log_2 \left(\frac{w_i}{\bar{w}_g} \right),$$

where $\bar{w}_g = \exp(\frac{1}{K} \sum_j \log w_j) = (\prod_j w_j)^{1/K}$ is the geometric mean. When all w_i are equal, $\log_2(w_i/\bar{w}_g) = 0$ and the optimal allocation is uniform.

The clipped variant ($B_i \in [0, B_{\text{max}}]$) is standard water-filling: solve unconstrained, identify saturated coordinates, fix them at boundary, redistribute residual budget among unsaturated coordinates by re-solving the reduced problem. \square

B.7 Proof of Corollary 5.6

The proof is a deterministic relative-error transfer lemma followed by an empirical-second-moment concentration bound; their composition gives the stated rate.

Relative-error transfer.

Lemma B.8 (Relative-error transfer). *Let $w_1, \dots, w_K > 0$ and $\hat{w}_1, \dots, \hat{w}_K > 0$ satisfy $|\hat{w}_i - w_i| \leq \eta w_i$ for all i , with $\eta \leq 1/2$. Let B^*, \hat{B}^* be the unclipped water-filling allocations of Theorem 5.5 computed from w and \hat{w} respectively. Then*

$$F(\hat{B}^*) \leq (1 + 2\eta + 4\eta^2) F(B^*).$$

Proof. Substituting $\hat{B}_i^* = B_{\text{tot}}/K + (V/2) \log_2(\hat{w}_i/\hat{w}_g)$ into the per-node objective term gives

$$w_i \cdot 2^{-2\hat{B}_i^*/V} = w_i \cdot 2^{-2B_{\text{tot}}/(KV)} \cdot \frac{\hat{w}_g}{\hat{w}_i}.$$

Comparing with $w_i \cdot 2^{-2B_i^*/V} = \bar{w}_g \cdot 2^{-2B_{\text{tot}}/(KV)}$ from the proof of Theorem 5.5 in § B.6,

$$\frac{F(\hat{B}^*)}{F(B^*)} = \frac{\sum_i w_i (\hat{w}_g/\hat{w}_i)}{K \bar{w}_g} = \frac{1}{K} \sum_{i=1}^K \frac{w_i}{\hat{w}_i} \cdot \frac{\hat{w}_g}{\bar{w}_g}.$$

Under $|\hat{w}_i - w_i| \leq \eta w_i$ with $\eta \leq 1/2$ we have $\hat{w}_i \geq (1 - \eta)w_i \geq \frac{1}{2}w_i > 0$, and a Taylor expansion of $1/(1 - \eta)$ gives $w_i/\hat{w}_i \leq 1/(1 - \eta) \leq 1 + \eta + 2\eta^2$. The geometric mean factor is bounded by AM–GM: $\hat{w}_g/\bar{w}_g = \prod_i (\hat{w}_i/w_i)^{1/K} \leq 1 + \eta$. Multiplying,

$$\frac{F(\hat{B}^*)}{F(B^*)} \leq (1 + \eta + 2\eta^2)(1 + \eta) = 1 + 2\eta + 3\eta^2 + 2\eta^3 \leq 1 + 2\eta + 4\eta^2,$$

the last inequality using $2\eta^3 \leq \eta^2$ for $\eta \leq 1/2$. □

Concentration of the empirical-second-moment estimator.

Lemma B.9 (Concentration of the empirical-second-moment estimator). *Under Assumption 5.1, let $b_0 := B_{\text{tot}}/(KV)$ denote the warm-up per-coordinate bit budget and define the post-quantization range*

$$R_\ell := L_\ell \cdot (1 + 2^{-b_0}) = L_\ell \cdot (1 + 2^{-B_{\text{tot}}/(KV)}).$$

With probability at least $1 - \delta$,

$$|\hat{w}_i - w_i| \leq R_\ell^2 \sqrt{\frac{\log(2K/\delta)}{2mT_0}} \quad \text{for all } i \in \{1, \dots, K\}.$$

Proof. Define block averages $S_{i,t,l} := \frac{1}{V} \sum_{v=1}^V (\tilde{\ell}_{i,v}^{(l,t)})^2$ for $t \in \{1, \dots, T_0\}$, $l \in \{1, \dots, m\}$. By Assumption 5.1, the input logits are clipped to $[-L_\ell, L_\ell]$ before quantization, but a subtractively dithered uniform quantizer with bin width $\Delta = 2L_\ell/2^{b_0}$ may produce reconstructed values $\tilde{\ell}_{i,v}^{(l,t)}$ extending up to $\pm\Delta/2$ beyond the input clip range, i.e., $\tilde{\ell}_{i,v}^{(l,t)} \in [-R_\ell, R_\ell]$ with $R_\ell = L_\ell(1 + 2^{-b_0})$. Hence $S_{i,t,l} \in [0, R_\ell^2]$. The probe contexts are i.i.d. across l by the probe draw, and warm-up rounds use the uniform pilot allocation independent of any feedback (the warm-up encoder $f_i^{(t)}$ depends only on \mathcal{D}_i , X_{probe} , and the round- t dither $U_i^{(t)}$, and dither is independent across (t, l)). Hence $\{S_{i,t,l}\}_{(t,l)}$ are i.i.d. within node i with mean $w_i = \mathbb{E}[\frac{1}{V} \|\tilde{\ell}_i\|_2^2]$, and the estimator $\hat{w}_i = (T_0 m)^{-1} \sum_{t,l} S_{i,t,l}$ is the sample mean of $T_0 m$ such bounded i.i.d. variables. Hoeffding's inequality applied to range R_ℓ^2 gives, for each i separately,

$$\Pr \left[|\hat{w}_i - w_i| \geq R_\ell^2 \sqrt{\frac{\log(2K/\delta)}{2mT_0}} \right] \leq \delta/K.$$

A union bound across the K nodes converts this into the stated high-probability claim. □

Composition. Set $\eta := (R_\ell^2/w_{\min})\sqrt{\log(2K/\delta)/(2mT_0)}$ and assume the warm-up sample size mT_0 is large enough that $\eta \leq 1/2$ (otherwise the bound is vacuous). Lemma B.9 gives $|\hat{w}_i - w_i| \leq \eta w_i$ uniformly in i with probability $\geq 1 - \delta$. Lemma B.8 then yields $F(\hat{B}^*) \leq (1 + 2\eta + 4\eta^2) F(B^*) \leq (1 + 3\eta)F(B^*)$ for $\eta \leq 1/4$, and

$$3\eta = \frac{3R_\ell^2}{w_{\min}} \sqrt{\frac{\log(2K/\delta)}{2mT_0}} \leq c_{\text{ad}} \sqrt{\log(K/\delta)/(mT_0)}, \quad c_{\text{ad}} := \frac{3R_\ell^2}{w_{\min}} \sqrt{\frac{\log 2+1}{2}},$$

using $\log(2K/\delta) \leq (\log 2 + 1) \log(K/\delta)$ for $K/\delta \geq e$. The post-quantization range R_ℓ exceeds the input clip L_ℓ by a factor $(1 + 2^{-b_0})$ that is bounded by 2 for any $b_0 \geq 0$ (and approaches 1 as the warm-up bit budget grows); the constant c_{ad} is therefore at most $4\times$ what it would be under the (incorrect) assumption $R_\ell = L_\ell$, and the $1 + O(\sqrt{\log(K/\delta)/(mT_0)})$ relative-suboptimality rate of Corollary 5.6 is unchanged. \square